IMPACT OF LANDAU OCTUPOLES ON THE TRANSVERSE BEAM HALO DISTRIBUTION IN THE LHC*

P. Hermes†, C. Maccani, D. Veres,
European Organization for Nuclear Research, Geneva, Switzerland
M. Rakic, École Polytechnique Fédérale de Lausanne, Lausanne, Switzerland

Abstract

The distribution of beam halo particles in the Large Hadron Collider (LHC) is affected by non-linear fields, in particular by the Landau octupoles used to provide tune spread for beam stabilization. These elements introduce amplitude-dependent tune shifts that deform the transverse phase-space and may alter the steady-state halo population. In this study, tracking simulations are performed to quantify the change of particle amplitude for different octupole settings, without beam-beam interactions, and to investigate whether such non-linear effects could contribute to the variations observed in different measurements. The analysis provides a first assessment of the impact of non-linearities on the observed beam halo characteristics in the LHC. The results indicate that particle amplitudes can be significantly enhanced by non-linearities, with consequences on the halo measured in collimator scrapings.

INTRODUCTION

The transverse beam halo in the LHC is routinely characterized through collimator scraping measurements, in which a collimator jaw is moved transversely into the beam and the resulting particle losses are recorded as a function of jaw position. For a Gaussian beam, the cumulative halo content removed by scraping to a jaw position of a_{cut} (in units of the beam size $\sigma = \sqrt{\varepsilon\beta}$) should follow the Rayleigh distribution, predicting approximately 1.1% for $a_{\mathrm{cut}} = 3$. Scraping measurements in the LHC consistently reveal populations exceeding this expectation [1–4], with strong variations across measurements whose origin is not fully understood.

In the LHC, sextupolar fields can drive third-order resonances, while the Landau octupoles introduce amplitude-dependent tune shifts [5]; in the vicinity of a resonance, these effects result in the distortion of the phase space structure. Collimator jaws intercept particles based on their physical transverse displacement at the collimator location, thus the measured halo population depends on the maximum displacement a particle can reach. In a nonlinear lattice, the latter can differ substantially from the linear expectation.

In this contribution, we develop a method to quantify this non-linear amplitude excursion in simulations and apply it to the 2025 LHC configuration. Results are presented for the horizontal plane of LHC Beam 1 (circulating clockwise), though the same methodology can be applied to all other planes. The results show a significant amplitude excursion, in particular for halo particles, with a strong asymmetry between the two collimator jaws.

* Research supported by the HL-LHC project
† pascal.hermes@cern.ch

THE NONLINEAR AMPLITUDE EXCURSION MAP

Let us define the generalized horizontal amplitude of a particle as $\mathscr{R}_x(\psi_x) = \sqrt{X^2 + P_X^2}$, where $X = x/\sqrt{\beta_x}$ and $P_X = (\alpha_x x + \beta_x x')/\sqrt{\beta_x}$ are the Courant-Snyder normalized coordinates, and $\psi_x = -\arctan(P_X/X)$ is the betatron phase. In the following, all quantities refer to the horizontal plane; the plane index is omitted except where needed for clarity.

In a linear machine, $\mathscr{R} = \sqrt{2J}$ is a constant of motion, where J is the linear betatron action. In a nonlinear lattice, $\mathscr{R}(\psi)$ varies with phase: a particle inserted into a lattice at $(X_0, P_{X,0})$, with initial amplitude $\mathscr{R}_i = \sqrt{X_0^2 + P_{X,0}^2}$, can have a different generalized amplitude as it moves along the ring. We express amplitudes in units of beam sigma via $a(\psi) = \mathscr{R}(\psi)/\sqrt{\varepsilon}$, with $a_i = \mathscr{R}_i/\sqrt{\varepsilon}$ the initial amplitude.

A collimator jaw intercepts particles whose transverse displacement X at the collimator location exceeds the jaw edge position a_{cut}. In a linear machine, the maximum displacement is $X_{\max} = a_i$, reached at $\psi = 0$ ($\psi = \pi$) for the left (right) jaw. In a nonlinear lattice, the maximum displacement depends on the full initial condition $(X_0, P_{X,0})$, not only on $\mathscr{R}_i$. Nonlinearities can therefore drive a particle into the jaw even if $a_i < a_{\mathrm{cut}}$. We quantify this effect through the amplitude enhancement $\Delta a^{\pm}$, defined as

$$\Delta a^{\pm}(X_0, P_{X,0}, Y_0, P_{Y,0}, \Delta p/p, s) = \frac{\sup_{n\geq 1}(\pm X^{(n)})}{\sqrt{\varepsilon}} - a_i, \tag{1}$$

where $X^{(n)}$ is the horizontal normalized coordinate on turn n, and + (−) corresponds to the left (right) side in the moving right-handed coordinate system. In a linear machine, the quantity $\Delta a^{\pm}$ always equals 0. In a nonlinear lattice, phase space distortion shifts the phase at which the maximum displacement occurs, and $\Delta a^{\pm}$ can differ substantially from zero.

For a given direction ($\pm$), fixed vertical conditions $(Y_0, P_{Y,0})$, constant $\Delta p/p$, and lattice position s, $\Delta a^{\pm}$ reduces to a two-dimensional scalar field over $(X_0, P_{X,0})$, referred to as the *Nonlinear Amplitude Enhancement Map* (NAEM). Regions of positive $\Delta a^{\pm}$ indicate trajectories that carry the particle beyond its linear amplitude boundary. The spatial structure of the NAEM is a direct fingerprint of the nonlinear response of the accelerator lattice. Note that the NAEM is defined with respect to a reference emittance but

can be easily scaled to any other emittance without need of a recomputation.

SIMULATION SETUP

The NAEM is computed from symplectic tracking simulations performed on GPUs with the XSUITE code [6], using the 2025 LHC optics at 6.8 TeV corresponding to end-of-luminosity-levelling conditions with $\beta^* = 60/18$ cm. Beam-beam effects are not included. Tracking starts at the horizontal primary collimator (TCP), and tunes and chromaticities are matched to target values via quadrupole and sextupole strengths, yielding $Q_x/Q_y = 62.31/60.32$ and $Q'_x = Q'_y \in \{0, 10, 20\}$.

A uniform 100×100 grid of initial conditions $(X_0, P_{X,0})$ is sampled over $[-5\sqrt{\varepsilon}, +5\sqrt{\varepsilon}]$ in each normalized coordinate, corresponding to $\pm 5\sigma$ at the nominal emittance $\varepsilon_n = 3.5\,\mu$m rad. All particles are assumed to be on-momentum. Each particle is assigned a fixed initial vertical amplitude a_y at betatron phase $\psi_y = 0$. Tracking is performed for $N = 500$ turns, sufficient for each particle to sample its accessible phase space at least once. The horizontal normalized coordinate $X^{(n)}$ is recorded turn by turn to evaluate $\Delta a^{\pm}$ via Eq. (1). Particles lost during tracking are excluded from the analysis.

Two scenarios are studied for the vertical amplitude: $a_y = 0$ (no vertical action, fully factorizable distribution) and the fully non-factorizable case $a_y = a_x$, in which each particle carries equal horizontal and vertical generalized amplitude. The octupole current is scanned from -570 to $+570$ A in steps of 100 A. Each study requires approximately 8 minutes of GPU time when using a NVIDIA T4 GPU (168 GB RAM, and 28 vCPUs).

RESULTS

Figure 1 shows the NAEM for the left and right jaw, for $a_y = 0$ and $a_y = a_x$, at two octupole currents. All maps exhibit a characteristic three-fold symmetry, consistent with the proximity of the nominal LHC working point to the third-order resonance line. For a given configuration, the Landau octupoles modify small features of the local amplitude of the NAEM but not its global structure.

For the left side, Δa^+ is predominantly positive across phase space: most particles reach a larger maximum displacement than the linear expectation. The enhancement is substantially amplified in the non-factorizable case $a_y = a_x$, reflecting the inter-plane coupling of the non-linear motion through the machine. On the right side, the picture is qualitatively different: Δa^- is predominantly negative for $a_y = 0$, indicating that particles reach a *smaller* maximum negative displacement than in a linear machine. Only for $a_y = a_x$ does the right jaw also show a net positive enhancement.

Figure 2 shows the phase-space-averaged amplitude increase $\langle \Delta a^{\pm} \rangle (a_i)$, obtained by averaging $\Delta a^{\pm}$ over all grid points in each amplitude annulus. This projection condenses the two-dimensional NAEM into a single curve per configuration, directly quantifying the mean amplitude excursion

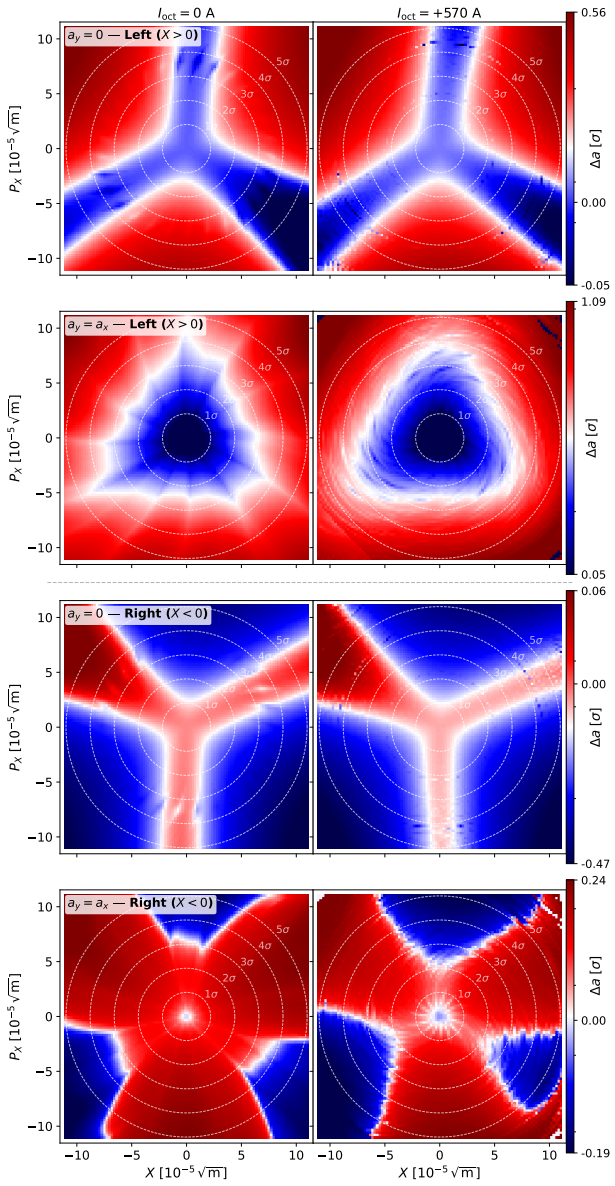

Figure 1: Absolute amplitude increase $\Delta a^{\pm}(X_0, P_{X,0})$ for the 2025 LHC configuration at 6.8 TeV, $\beta^* = 60/18$ cm, $\varepsilon_n = 3.5\,\mu$m rad, $Q_x/Q_y = 62.31/60.32$, $\Delta Q = 0$. Left side (positive X): $a_y = 0$ (row 1) and $a_y = a_x$ (row 2). Right side (negative X): $a_y = 0$ (row 3) and $a_y = a_x$ (row 4). Columns: $I_{\text{oct}} = 0$ A (left) and $I_{\text{oct}} = +570$ A (right). White dashed circles indicate integer-σ amplitudes. Note the different colour scales per row.

as a function of initial amplitude. For the left side, $\langle \Delta a^+ \rangle$ is positive and grows with a_i, reaching up to 0.6 σ near 5 σ for $a_y = a_x$. For the right side, $\langle \Delta a^- \rangle$ remains negative for $a_y = 0$, revealing a fundamental asymmetry between scraping with the left and right jaw. For $a_y = a_x$, the right jaw also yields a positive mean excursion.

While the amplitude excursion is insensitive to octupole current in the fully factorizable case, it varies slightly in the non-factorizable case. For example, at an initial amplitude of $a_x = a_y = 5\,\sigma$ when scraping with the right jaw, we observe

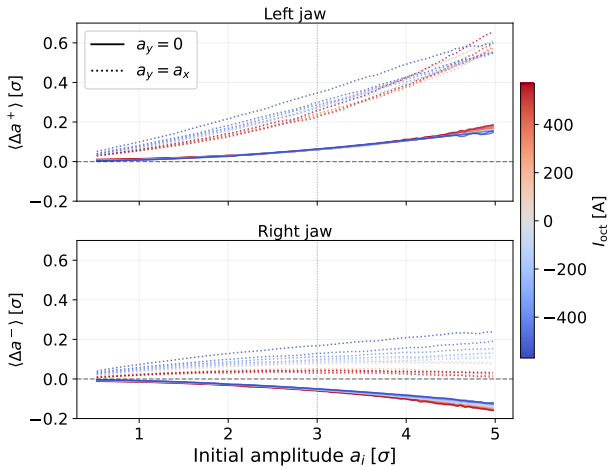

Figure 2: Phase-space-averaged amplitude increase $\langle \Delta a^{\pm} \rangle (a_i)$ as a function of initial amplitude. Octupole current encoded by colour (blue: −570 A, red: +570 A); linestyle distinguishes $a_y = 0$ (solid) and $a_y = a_x$ (dotted). The lines show the average across the chromaticities studied, $\Delta Q \in \{0, 10, 20\}$. Top: left jaw; bottom: right jaw.

$\langle \Delta a^- \rangle \approx 0$ for strong negative octupole currents, while strong positive currents lead to an amplitude enhancement of more than $0.2\,\sigma$.

OUTLOOK

The NAEM provides the foundation for a quantitative prediction of the halo content observed in scraping measurements. Building on the results presented here, we will, in a next step, fold the NAEM with a two-dimensional Gaussian beam distribution, yielding the halo content above a_{cut} as:

$$N^{\pm}(a_{\mathrm{cut}}) = \frac{1}{2\pi\varepsilon} \iint_{\Omega^{\pm}} \exp\left(-\frac{\mathscr{R}^2}{2\varepsilon}\right) \mathrm{d}X\, \mathrm{d}P_X, \qquad (2)$$

where $\Omega^{\pm}$ is the region of initial conditions intercepted by the left (+) or right (−) jaw during tracking. In a linear machine, particle amplitudes are conserved and $\Omega^{\pm} = \{a_i > a_{\mathrm{cut}}\}$ for both jaws, so Eq. (2) reduces to the Rayleigh function $\bar{N} = e^{-a_{\mathrm{cut}}^2/2}$, predicting the 1.1% above $a_{\mathrm{cut}} = 3\sigma$, referred to previously. The intercepted region becomes $\Omega^{\pm} = \{a_i + \Delta a^{\pm} > a_{\mathrm{cut}}\}$.

In practice, the expected halo taking into account the nonlinear change of $\Omega^{\pm}$ is assessed using the discrete estimator

$$N^{\pm}(a_{\mathrm{cut}}) \approx \frac{1}{\mathscr{W}} \sum_{\substack{i,j \\ a_i + \Delta a^{\pm}_{ij} > a_{\mathrm{cut}}}} \exp\left(-\frac{X_i^2 + P_{X,j}^2}{2\varepsilon}\right), \qquad (3)$$

where $\Delta a^{\pm}_{ij}$ is the NAEM evaluated at grid point $(X_i, P_{X,j})$ and $\mathscr{W}$ is the total Gaussian weight. This directly yields the predicted scraped fraction as a function of jaw position.

To compare with measurement, the beam-based alignment procedure must also be simulated, because it directly influences the actual a_{cut}. In the experiment, both jaws are moved inward independently until a loss spike is detected at the BLM; the midpoint of the two touch positions defines the beam centre, and the half-gap sets the betatron cut a_{cut}. In the simulation, the positions that would be obtained from such a beam based alignment is unknown, but can be approximated as the amplitude at which a prescribed fraction of the Gaussian-weighted beam is intercepted by that jaw, as determined from the NAEM. Since Δa^+ and Δa^- are in general different, the two collimator positions after alignment are shifted asymmetrically by the nonlinear dynamics, displacing the inferred beam centre from the true centre. This introduces a bias in a_{cut} that propagates into the halo estimate and will, in general, differ between the two jaws.

Once the alignment is simulated, the cumulative scraped fraction can be evaluated via Eq. (3). The result is a direct quantitative prediction of the halo content in the presence of non-linearities.

The model is going to be further extended to incorporate a full four-dimensional phase space treatment, replacing the fixed vertical amplitude assumption with a proper integration over the vertical beam distribution. Including additional sources of nonlinear fields such as magnet field errors and beam-beam interactions will allow us to identify the impact of these effects on halo content and improve the general understanding of halo formation.

CONCLUSIONS

We have introduced the Nonlinear Amplitude Excursion Map (NAEM), a simulation-based method to quantify how nonlinear lattice elements modify the maximum amplitude a particle reaches at a collimator jaw. Applied to the 2025 LHC configuration at 6.8 TeV, the NAEM reveals a strong asymmetry: the left side is exposed to a predominantly positive amplitude excursion, while for the right side the excursion is predominantly negative in the fully factorizable case. The excursion grows with initial amplitude and is significantly amplified in the non-factorizable case $a_y = a_x$, where interplane coupling drives larger excursions on both jaws. The octupole current modulates the excursion, particularly in the non-factorizable regime, while chromaticity plays a minor role.

Based on the findings presented in this contribution, we hypothesise that the magnitude of the observed halo excess above the Rayleigh expectation, as well as its variation across measurements, may be partly attributed to the nonlinear amplitude excursion driven by the machine lattice, which motivates further studies.

REFERENCES

[1] F. Burkart *et al.*, "Halo Scrapings with Collimators in the LHC", in *Proc. IPAC'11*, San Sebastian, Spain, Sep. 2011, pp. 3756–3758. https://jacow.org/IPAC2011/papers/THPZ030.pdf

[2] G. Valentino *et al.*, "Halo Scraping, Diffusion and Repopulation MD", CERN-ATS-Note-2012-074 MD, 2012. http://cds.cern.ch/record/1480603

[3] A. Gorzawski *et al.*, "Probing LHC Halo Dynamics Using Collimator Loss Rates at 6.5 TeV", *Phys. Rev. Spec. Top. Accel. Beams*, vol. 23, p. 044802, 2020. doi:10.1103/PhysRevAccelBeams.23.044802

[4] M. Rakic, "Limitations from the transverse beam halo at the high luminosity LHC and its mitigation", PhD Thesis, École Polytechnique Fédérale de Lausanne, Lausanne, 2026. doi:10.5075/epfl-thesis-12223

[5] O. S. Brüning *et al.* (editors), "LHC design report v.1 : the LHC main ring", CERN-2004-003-V1, 2004.

[6] G. Iadarola *et al.*, "Xsuite: An Integrated Beam Physics Simulation Framework", in *Proc. HB'23*, Geneva, Switzerland, Oct. 2023, pp. 73–80. doi:10.18429/JACoW-HB2023-TUA2I1